Review and Trends of Thermoelectric Generator Heat Recovery in Automotive Applications

Romina Rodriguez, *Student Member, IEEE*, Matthias Preindl, *Senior Member, IEEE*, James S. Cotton, and Ali Emadi, *Fellow, IEEE*

***Abstract*—Automotive vehicles with internal combustion engines, such as conventional gasoline and electric hybrid vehicles, exhibit inherent irreversibilities that hinder them from achieving high efficiencies. These irreversibilities manifest themselves in the form of thermal losses in the engine and contribute to the total energy consumption in the transportation sector. Waste heat recovery is a method to increase the overall fuel efficiency of vehicles by recovering thermal energy that would be lost from the engine to the environment and converting it to useful energy for the vehicle. In the past years, thermoelectric generators have been intensively investigated for waste heat recovery in vehicles because they are solid-state devices that convert heat directly into electricity and hence have no moving parts, operate quietly, are relatively small, and require low maintenance. This paper presents a review of the literature on waste heat recovery in vehicles through the implementation of thermoelectric generators. First, potential sources or locations in a vehicle for waste heat recovery are presented. Second, the available thermoelectric technology for vehicle applications is reviewed. Then, the components required to create a waste heat recovery system are discussed. The approach for modeling thermoelectric generators to predict the power output is then considered. Finally, experimental investigations by researchers are presented as well as the future trends observed for waste recovery via thermoelectrics.**

***Index Terms*—Automotive, maximum power point tracking (MPPT), thermoelectric generator (TEG), waste heat recovery.**

I. Introduction

IN RESPONSE to alarming climate change and global warming, the Paris Agreement set a goal of maintaining the global average temperature to 2° C below pre-industrial revolution levels. To achieve this target, the International Energy Agency (IEA) suggests limiting the total greenhouse gas emissions to 1170 gigatonnes of equivalent carbon dioxide ($GtCO_2$) between 2015 to 2100 [1]. Considering the transportation sector accounts for 23% of the world's green house gas emissions, vehicle electrification is crucial [1]. In 2016 only 0.2% of the world's passenger vehicles were electrified, but Bloomberg New Energy Finance predicts that 33% [2] of the vehicle fleet will be electric by 2040 and the IEA greenhouse gas limitations require 60% of all vehicles to be electrified by 2060 to meet the Paris Agreement goal. Electric vehicles (EV) are considered battery-electric vehicles (BEVs), plug-in hybrid vehicles (PHEVs) and fuel cell vehicles (FCEVs) which means that a fraction of these EVs will include an internal combustion engine (ICE). Therefore, not only will 40% of the future vehicle fleet (this number may be larger as there is no implemented policy that mandates the electrification of vehicles worldwide) operate only with ICE's but also a percentage of the 60% of electrified vehicles will include an ICE (such as PHEVs).

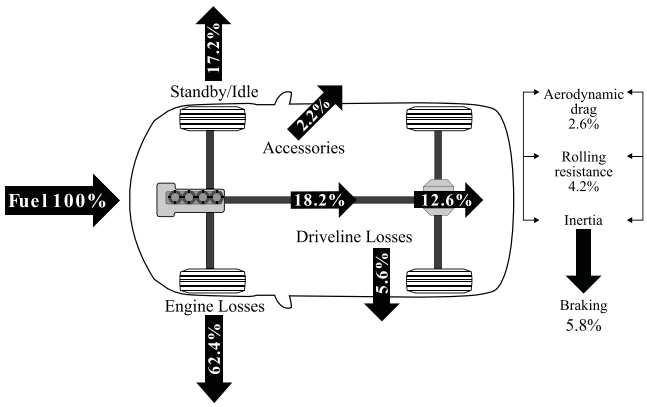

Fig. 1. Fuel energy losses in vehicle (values from CA Energy Commission).

The problem with the future vehicle fleet consisting of a large number of ICE's is their hindrance by the Carnot efficiency- heat engine operating between two temperature points. There are inherent irreversibilities during the operation of ICE vehicles that prevent them from running at higher efficiencies; it is physically impossible to achieve the efficiencies of an electric motor. Approximately 20% of fuel energy in an ICE is converted to useful work while the rest is lost through friction, the cooling system and the exhaust gases as observed in Fig. 1. Therefore, to increase the overall fuel economy of an ICE, waste heat recovery is necessary.

Waste heat recovery is the process of converting energy that would end up in the environment as heat and converting it to work such as electricity. In recent years, there has been increasing interest in research that investigates waste heat recovery in vehicles [3]–[6] through the use of thermoelectric generators (TEGs). Thermoelectric generators are solid state devices

Manuscript received July 11, 2018; revised February 6, 2019; accepted March 17, 2019. Date of publication March 28, 2019; date of current version June 18, 2019. This work was supported by the Canada Excellence Research Chairs (CERC) Program and the Natural Sciences and Engineering Research Council of Canada (NSERC). The review of this paper was coordinated by Prof. M. Kazerani. *(Corresponding author: Romina Rodriguez.)*

R. Rodriguez, J. S. Cotton, and A. Emadi are with the Department of Mechanical Engineering, McMaster University, Hamilton, ON L8S 4L8, Canada (e-mail: romina@mcmaster.ca; cottonjs@mcmaster.ca; emadi@mcmaster.ca).

M. Preindl is with the Department of Electrical Engineering, Columbia University, New York, NY 10027 USA (e-mail: matthias.preindl@gmail.com).

Digital Object Identifier 10.1109/TVT.2019.2908150

that convert thermal energy directly to electrical energy due to the Seebeck effect. Additional advantages are their small size, quiet operation and low maintenance required. Although different technologies have been investigated for waste heat recovery in vehicles, such as organic Rankine cycle or turbocharger, the challenge lies in the operation of these technologies. Vehicle operation is dynamic- the losses that are generated vary depending on driving conditions. A system which recovers energy that is lost throughout the vehicle needs to quickly respond to these variable operating conditions. Since thermoelectric generators have no moving parts, or working fluids such as refrigerants, they can handle these dynamics and still operate with minor impact to the operation of the vehicle.

This paper presents an overview of waste heat recovery in vehicles with thermoelectric generators. First, the locations of potential waste heat recovery in automotive ICE's are presented. In the second section, thermoelectric generator technology is reviewed as well as the working principle behind TEGs. Then, the waste heat recovery system components are explained. In section V, the approach to modeling TEG waste heat recovery systems is described. Finally, the design of thermoelectric waste heat recovery systems through modeling and experimental work performed is presented, as well as future trends in this field.

II. Energy Sources in Vehicles

During vehicle operation, thermal losses are a result of fuel energy conversion to mechanical energy by an ICE due to system inefficiencies, as well as thermodynamic limits i.e. Carnot efficiency. The Carnot efficiency is the theoretical maximum efficiency a heat engine can achieve when operating between two temperatures and for ICE it is $\sim$70% [7]. These losses are potential sources of "free" energy for waste heat recovery- considered "free" since the energy would otherwise end up in the environment in the form of heat. There are different locations of waste heat that have the potential for recovery in a vehicle, whether it be an ICE or hybrid car. The maximum power available, $Q_{\max}$ [W], for recovery can be calculated as [8]

$$Q_{\max} = \dot{m} C_p (T_f - T_c) \tag{1}$$

where $\dot{m}$ [kg/s] is the fluid mass flow rate, C_p [J/kg-K] is the fluid's specific heat, T_f [K] is the temperature of the fluid source, and T_c (typically ambient) is the reference temperature the fluid can be cooled down to.

ICE include both spark-ignition (SI) and diesel engines. 17–26% and 16–35% of the fuel energy is lost to the engine coolant for SI engines and diesel engines, respectively. While 34–45% and 22–35% of the fuel energy is lost to the exhaust gases for SI engines and diesel engines, respectively at maximum power [9]. The magnitude of the thermal losses depends on the engine size and the driving conditions. Table I provides approximate source temperatures for various locations where energy can be recovered. The high temperatures of the exhaust gases make the exhaust system the most researched area for waste heat recovery in a car. As exhaust gases move downstream towards the tailpipe, the temperature drops as losses occur to ambient. Typically, the location for waste heat recovery along the exhaust system is after the catalytic converter (CC) to avoid interfering with the minimum temperature required for the catalyst to reduce emissions. The radiator is another potential location for waste heat recovery; the coolant used to maintain the engine block below critical temperatures, is cooled in the radiator. Although the radiator has the lowest temperatures, a benefit is that a heat exchanger already exists for extracting the energy from the coolant hence, converting this energy has minimal impact. The Exhaust Gas Recirculation (EGR) cooler is another option as well, since the exhaust gases that are recirculated back to the cylinder for NOx emissions reduction, require cooling before injection and therefore has the same benefits as the radiator.

TABLE I
Approximate Fluid Temperatures of Heat Source

Location	Temperature [°C]	Reference
Exhaust manifold [a]	550 - 790	[10]
Catalytic converter [a]	320 - 520	[10]
Radiator	90 - 120	[11]
EGR	540 - 770	[12]

[a] Diesel engines are 100–200 degrees lower.

TABLE II
Approximate Fluid Flow Rates of Heat Source

Fluid	Flow Rate [kg/s]	Reference
Exhaust gas (gasoline)	0.01 - 0.045 [a] ; 0.01 - 0.11 [b]	[16];[17]
Exhaust gas (diesel)	0.1 - 0.4 [c]	[18]
Coolant	1.84 - 3.13 [d]	[15]

[a] 190 kW engine, FTP drive cycle.
[b] 180 kW engine, 120–140 kmh highway driving.
[c] 290 kW engine, reduced Paris-Lille drive cycle.
[d] Calculated for 100 kW engine.

The potential for waste heat recovery not only depends on the temperature of the fluid source but also its mass flow rate. Approximate mass flow rate values are found in Table II. The mass flow rate of the exhaust gases varies rapidly during a drive cycle and more aggressive driving conditions result in higher mass flow rates. Typically, 20-50% of the exhaust gases are recirculated back to the engine cylinder in EGR applications, depending on the engine size and cylinder charge temperature control strategy [13], [14]. Compared to the coolant flow rates, the exhaust mass flow rates are a magnitude lower. According to [15], advanced engines require 1–1.7 L/min/kW, which results in high mass flow rates for the coolant. Even if electrical pumps were used in all ICE vehicles instead of mechanical belt-driven pumps, 1 L/min/kW is necessary to meet the cooling demands of the engine block.

When choosing the location for waste heat recovery both temperature and mass flow rate of the system need to be taken into account. Next, the thermoelectric technology that can be used in these various locations is presented.

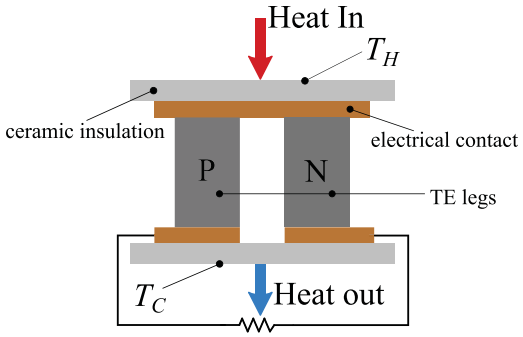

Fig. 2. Thermoelectric generator schematic.

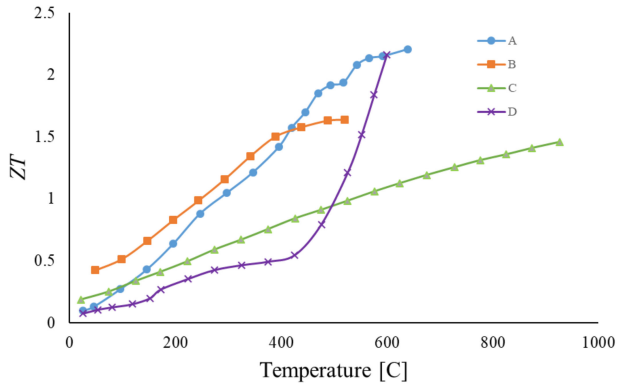

Fig. 3. ZT as a function of temperature for various TE materials. (a) p-type PbTe endotaxially nanostructured with SrTe [23]. (b) Skutterudite $Co_{23.4}Sb_{69.1}Si_{1.5}Te_{6.0}$ [24]. (c) p-type FeNbSb half-Heusler [25]. (d) p-type polycrystalline $Sn_{.95}Se$ [26].

III. Thermoelectric Generator Technology

Thermoelectric generators are solid state devices that work through the Seebeck principle. A positive-doped (p-type) semiconductor is connected to a negative-doped (n-type) semiconductor to create a thermoelectric (TE) junction, referred to as a p-n couple. When a temperature difference is applied across the TE junction, an electromotive force is induced known as the Seebeck effect and if an electrical load is connected, current is allowed to flow. Hence, they are considered generators due to their direct conversion of thermal energy to electrical energy. If the reverse occurs, i.e. electricity is supplied, then heat will flow in the opposite direction from cold to hot junction. This phenomenon is known as the Peltier effect and the device that operates with a power input is considered a thermoelectric cooler. The open circuit voltage, E [V], generated across the junction when a temperature difference is applied can be defined as [19]

$$E = \alpha \Delta T \tag{2}$$

where α [V/K] is the Seebeck coefficient, a temperature-dependent material property and ΔT [K] is the temperature difference across the junction. A TEG *module* consists of many p-n couples connected electrically in series and requires electrical insulation from the heat source (usually a ceramic). The hot side temperature of the TEG module is T_H and the cold side temperature is T_C, as shown in Fig. 2.

The efficiency of a p-n couple, defined as the electric power output divided by the heat input, is a function of: the temperature difference, electrical load and the material properties (α, σ and k). Since thermoelectric performance depends on these material properties, the figure of merit Z was created to evaluate and compare TE materials [20] and is widely accepted in the literature. However, the non-dimensional figure of merit ZT is more commonly used and is defined as [20]

$$ZT = \frac{\alpha^2 \sigma}{k} T \tag{3}$$

where σ [S/m] is the electrical conductivity, k [W/m-K] is the thermal conductivity and T [K] is the temperature of the material. Large ZT values are desirable. Currently ZT values of common TE materials are in the range of 1–2. It is estimated that a 10% fuel efficiency gain can be achieved if a TEG has a ZT value of 2 [21], [22]. It should be noted that in the literature, maximum ZT values are reported when researching TE materials, however, they vary with temperature. This is pointed out in Fig. 3, where ZT values are plotted as a function of temperature for various materials. The operating temperature of TEGs is dynamic in waste heat recovery applications for vehicles, therefore the average ZT value over the temperature range is important when considering material selection for the module for a specific application. Also, the ZT of the p-type and n-type of the same material are not equal over the operating temperature, hence this needs to also be considered when manufacturing a TEG module.

Commercially available TEGs have a $ZT \approx 1$ which results in a thermal to electrical conversion efficiency of $\sim$5%. The most commonly used material for TEGs is Bismuth Telluride (Bi_2Te_3), which has long been proven to work in low temperature settings ($<$250 °C). Lead Telluride (PbTe) and Silicon Germanium (SiGe) alloys are also commercially installed but are for higher temperature applications. Other prominent TE materials are TAGs (Te-Ag-Ge-Sb), half-Heusler and Skutterudites, which have been investigated materials for waste heat recovery in vehicles [3], [27], [28] and work best in the operation range of: PbTe ($\sim$500–600 °C), TAGs (200–500 °C), Half-Heusler (400–600 °C) and Skutterudite (500–800 °C). For the most part, TEG modules are manufactured using multiple TE materials.

Modules are manufactured from ingots which are cut into cubes (legs) for each p and n material. Due to their geometry, the p-n legs are connected to form a flat TEG module. Flat TEG modules are commercially available and the vast majority of researchers use flat TEGs for waste heat recovery systems in vehicles. Although [29] manufactured TEGs that appear cylindrical, p-n legs were placed in a circular formation to create a better interface between the exhaust gas heat exchanger and the TEGs. However, some have investigated other shapes such as annular TEGs. Instead of using p-n legs, p-n disks are used and potential advantages are easier integration with tubular heat exchangers that can fit more compactly in vehicle exhaust systems [30]–[32]. Fig. 4(a) shows a typical off-the-shelf TEG and Fig. 4(b) a prototype of a cylindrical TEG module. Annular TEGs are still in the research phase, as it has been difficult to manufacture the TE disks.

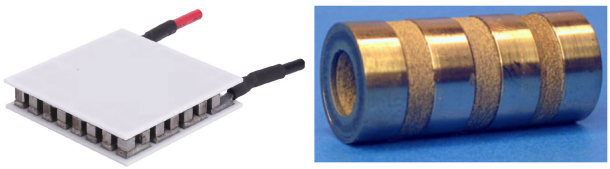

(a) (b)

Fig. 4. (a) Off-the-shelf flat TEG module. (b) Cylindrical TEG module concept [32].

As previously discussed, since the ZT value of the TE material changes with temperature, *segmented* TEGs have also been investigated. During operation of the TEG, the p-n legs will experience large temperature gradients, especially in vehicle applications. Therefore, using different TE materials in the direction of the heat flow (**Heat In** in Fig. 2) of the TEG is advantageous, making each TEG leg of *segmented* material. Each TE material along the TE leg is chosen for optimum performance at the temperature gradient. [33], [34] demonstrated through their computational modeling that TEG efficiency is enhanced through segmented TEGs, and could reach an efficiency higher than 10%. Crane *et al.* [35] manufactured segmented TEGs for recovering waste heat in the exhaust system of vehicles, and had a 100% increase in efficiency compared to a TEG without segmentation.

A. Electrical Characteristics

The electrical model of a TEG is seen in Fig. 8 b. The output voltage of the TEG, V_E [V], is calculated as [19]

$$V_E = E - IR_E \tag{4a}$$

$$= \alpha\left(T_H - T_C\right) - IR_E \tag{4b}$$

where I [A] is the current flowing through the TEG and R_E [Ohm] is the electrical internal resistance of the TEG. Hence the power output, P_E [W], of the TEG is defined as [19]

$$P_E = V_E I \tag{5a}$$

$$= \alpha\left(T_H - T_C\right) I - I^2 R_E \tag{5b}$$

For a fixed T_H and T_C, the maximum power output ($P_{\max}$) will occur when $IR_E = V_E$, which means that it occurs when V_E is half the open-circuit voltage ($E/2$), and $P_{\max} = \frac{\alpha\Delta T}{2} I$. A characterization of a TEG module, TEG1-12610–5.1 from TECTEG MFR is performed by maintaining T_C at a constant 35C and varying T_H between 100C and 250C; the results are shown in Fig. 5. V_E and P_E are plotted versus current, and the maximum power occurs at $E/2$ or half the short-circuit current, I_s. However, precaution should be taken when making this assumption when modeling the entire TEG waste heat recovery system, since taking into account the thermal resistance of the heat exchangers will shift I_s [36], i.e. I_s at the module level is not equal to I_s at the system level. An approximation for the maximum power is derived by noting that the max power occurs when $\frac{dP}{dI} = 0$ and (5b) becomes $\alpha\Delta T = 2IR$ which results in $I_{\max} = \frac{\alpha\Delta T}{2R}$ hence $P_{\max} = \frac{(\alpha\Delta T)^2}{4R_E}$.

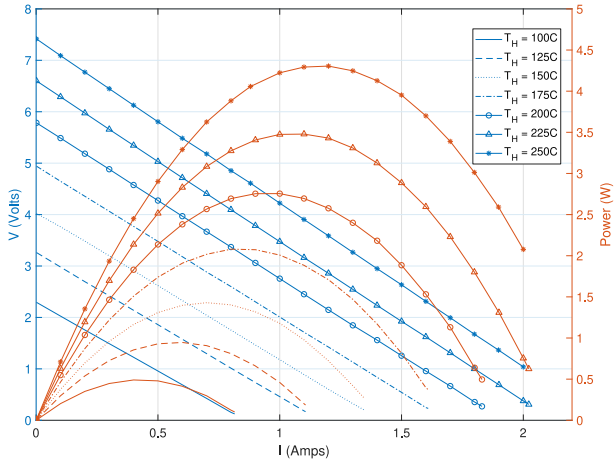

Fig. 5. Characterization of an off-the-shelf TEG module from TECTEG MFR. T_C is 35° C.

TABLE III
TEG MODULE CHARACTERIZED PROPERTIES

ΔT	α [V/K]	E [V]	R_E [OHM]
65	0.035	2.29	2.70
90	0.036	3.26	2.80
115	0.035	4.02	2.86
140	0.035	4.94	2.93
165	0.035	5.78	3.02
190	0.034	6.59	3.11
215	0.034	7.41	3.18

The Seebeck coefficient, open circuit voltage and R_E are all temperature-dependent. This can be observed from Table III, where the values were computed from the characterization performed at various temperature differences across the TEG module. The values reported are a function of temperature, which is influenced by the current flow and is further discussed in Section V-A1.

B. Thermal Characteristics

The thermal response of the TEG not only depends on the temperature difference applied across the thermoelectric junction but also on the Peltier heat and Joule heating. In general, since E ((2)) depends on the temperature difference, a large ΔT is desirable, hence the thermal resistance of the TEG should be large to achieve this. However, the Peltier effect negatively affects the TEG because the effective thermal resistance of the TEG decreases as current is increased through the TEG, i.e. ΔT decreases as current is increased. Due to the Peltier effect, heat is absorbed in the hot junction and emitted in the cold side. Joule heating as well reduces the total power produced by the system if (5b) is observed. Hence in general, TEG modules with lower operating currents are desirable. More detail regarding modeling of the physical phenomena of TEGs is presented in the modeling Section V-A1.

IV. TEG Waste Heat Recovery

Waste heat recovery (WHR) is the process of recovering energy that would be lost to the environment in the form of low-grade heat and converting it to high-grade electrical energy. Waste heat recovery can be implemented via TEGs by creating a temperature difference across the TEG module. In the previous section, the thermoelectric module was discussed but the other components necessary for a TEG WHR system are heat exchangers (HEXs). Heat exchangers are devices that transfer heat from one medium to another medium. The *hot* HEX extracts energy from the waste heat source and transfers it to T_H and the *cold* HEX completes the thermal circuit by cooling T_C. A schematic of a TEG WHR system is in Fig. 7. Once a temperature different is maintained across the TEG modules, a power conditioning unit is necessary to connect the output power of the TEG system to the vehicle.

A. Hot Side Heat Exchanger

Hot HEX's are necessary to extract thermal energy from the waste heat source in a vehicle and transfer it to a TEG. Preferably, T_H of the TEG should be as close as possible to the exhaust gas temperature to achieve a higher power output as expected from (5b). However, there is a temperature drop from the exhaust gas temperature to the temperature of the hot side of the TEG due to the thermal resistance of the hot HEX. The thermal resistance of a heat exchanger can be decreased by either increasing the surface area or the heat transfer coefficient of the HEX. The heat transfer coefficient, h (W/m^{2}K) is proportional to the Reynolds number (Re) which is dependent on the velocity of the gases. Since the majority of the research for TEG WHR systems in vehicles focuses on the exhaust system, low mass flow rates in the exhaust gases (Section II) hinder the achievement of a high heat transfer conductance. Wang *et al*. [6] showed that enhancing the hot TEG side heat transfer significantly increases the power output and efficiency of a TEG. Therefore, heat transfer enhancement techniques have mostly been studied for the hot HEX [37]–[41]. Passive enhancement techniques involve different geometries of fins, spiral inserts, baffles, etc. and their orientation placement in the heat exchanger have also been investigated. Niu *et al*. [40] suggested making the baffle angle adjustable for an automotive exhaust HEX to accommodate for various engine operation conditions thus increasing the power output of the TEG.

Typically, rectangular-duct HEX geometries have been investigated for harvesting the energy from the exhaust since they can compactly fit in the exhaust system [42]. Liu *et al*. [43] found that placing the HEX between the CC and the muffler resulted in the lowest pressure drop and uniform temperature distribution of the HEX surface. Pressure drop in the HEX is important to consider since the HEX is placed in the flow path of the exhaust gases and this creates a back pressure on the engine. In general heat transfer enhancement and pressure drop are related, so a trade-off is made when choosing the optimum heat exchanger design. For this reason, plate-fin heat exchangers are commonly used in the literature since they provide good heat transfer enhancement with acceptable pressure drop [18], [44]. Wang *et al*. [45] tested a plate-fin HEX filled with metal foam for enhancing TEG waste heat recovery and calculated a HEX efficiency of 83.56% with a total pumping power of .84W, for a total heat recovery of 285.3W.

B. Cold Side Heat Exchanger

The cold side HEX has the lowest thermal resistance (liquid-cooling) in the TEG WHR system and therefore is not a limiting factor in terms of heat transfer for the system. The majority of researchers have focused on liquid-cooling for the cold HEX due to the possibility of connection to the cooling system of the vehicle. Variations of cold-plate designs are used to cool the cold side of the TEG. Therefore, there is not much research in enhancement techniques for the cold HEX. Hendricks *et al*. found that the cold HEX thermal resistance needs to be 10–30 times less than the hot HEX to optimize the power output of the system [46]. Currently, there is limited research on the effect of the additional cooling load on the vehicle due to the cold HEX. However, for hybrid vehicles, this can be advantageous since there are heating loads that can no longer be met entirely by the engine during vehicle warm-up [47].

C. Power Conditioning Unit

Once the TEGs are exposed to a temperature difference, an electrical load is connected to the TEGs for power generation. The TEG WHR system will include several TEG modules and a decision is required regarding their electrical connection. The TEG modules can either be connected in series, in parallel or some combination of both depending on the desired output voltage. Studies have been conducted to understand how the electrical configuration affects the power output and as explained previously, the maximum power output of the TEG is of interest since the energy recovered is considered "free". Montecucco *et al*. [48] connected TEGs at different temperatures differences in series and also in parallel, to study the total power produced. As expected, the total power output was lower than the sum of the max power of each individual TEG, but the parallel TEG connection resulted in lower power produced than the series connection. Just like batteries, if a TEG is connected to another TEG with a different temperature difference (i.e. different, E), the TEG with the lower ΔT consumes power from the other TEG.

When TEGs with different temperature differences are connected electrically in series, there is a current mismatch at the maximum power point and when they are connected in parallel, the mismatch exists at the voltage. Ideally, each TEG would have its own converter to ensure the maximum power is transferred to the vehicle battery, but there is a trade-off between gain in power and added complexity. Hence a decision is required on the number of converters installed for rows or groups of TEGs. If TEGs are connected in parallel an advantage is that if one module fails, the rest continue to be operational but in general a larger current input is needed. At high current, larger diameter electrical leads for the TEG are necessary and Joule losses are higher. Therefore, TEGs are usually connected in series in the literature.

As explained previously and observed in Fig. 5, the power output from the TEG will change due to the operating conditions,

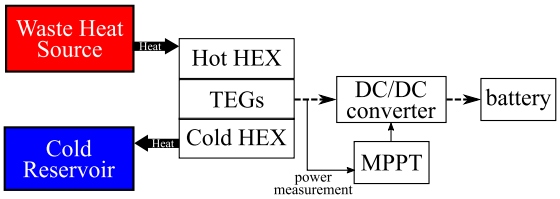

Fig. 6. TEG WHR system.

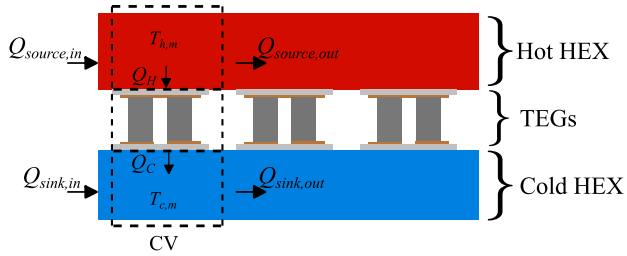

Fig. 7. TEG WHR thermal system model schematic.

hence maximum power point tracking (MPPT) is crucial to ensure the maximum available power is produced instantaneously. Different MPPT schemes are presented in the later section.

D. Additional Components/Considerations

Interface materials are essential for mounting the TEGs on the HEXs, thus reducing the thermal contact resistance and allowing better heat transfer. Thermal interface materials (TIMs) take the form of pastes, greases or sheets and these are placed between the TEG and the surface of the HEX. Thermal pastes harden at high temperatures; therefore, phase-change thermal pads may be considered for the hot side of the TEG as well as carbon-based TIMs [49]. Another factor that determines the contact resistance between the TEGs and HEXs is the applied pressure. The TEG WHR system assembly needs to be mechanically compressed to ensure maximum power output from the system. Wang *et al*. [50] experimentally showed that the output power increased by 61% when using thermal grease and the power increased by 33% when the pressure applied to the TEG was increased from 109 kPa to 765 kPa.

V. TEG Modeling

Accurate models are necessary to predict the operating conditions of a TEG WHR system and hence the power output potential. As previously discussed in Section III-B, the temperature difference across a TEG is also dependent on the electrical load applied. Therefore, to predict the operating temperatures of TEGs in a vehicle system, both the thermal and electrical characteristics must be modeled. The operating temperatures dictate the type of TEG module to choose for a system and the expected voltage generated (hence the power conditioning unit). Since the power output of a TEG varies with the electrical current (Fig. 5), MPPT schemes must be employed to ensure the maximum power is produced by the TEG at all operating points, thus increasing the overall energy recovered (integration of power with time) and system efficiency. A schematic for the complete TEG WHR system is shown in Fig. 6. To further understand how the power produced by the TEG depends on both thermal and electrical boundary conditions, a review of the thermal models found in the literature is presented, then the TEG WHR electrothermal governing equations are shown and maximum power point schemes are described.

A. Electro-Thermal Modeling

The majority of the research that explores modeling of thermoelectric generators focuses on the boundary conditions (working conditions) effects on TEG power generation and efficiency. Models simulate a single p-n couple (or a few) and parametric studies are performed by varying the length, area of the p-n pair, packing ratio, material properties etc. to observe its effect on power generation and efficiency. In general, the models can be categorized by the following assumptions: 1) fixed T_H and T_C temperature [51]–[53], 2) fixed heat source temperature and considers thermal resistance of the heat exchanger [54]–[56]. These models are important for providing guidelines for TEG module design that maximizes the power output of the module for specific applications (heat source temperature). The third, 3) considers exhaust flow direction [6], [18], [57]–[59] and is crucial to evaluate TEG performance in a real system. As the exhaust gas flows through the heat exchanger, energy will be transferred to the TEGs nearest to the inlet first and less energy is available for the TEGs downstream.

Waste heat recovery in vehicles is a dynamic operation and transient effects have also been considered by several researchers. Meng *et al*. [60] developed a 3D transient model of a TEG to capture the coupled energy and electrical potential phenomena. By varying T_H and T_C, the transient effects on power generation were investigated and it was concluded that the output power changes synchronously with load current but the thermal response is much slower. Guo *et al*. [61] presented a dynamic model of TEGs with finned heat exchangers for both the hot and cold side and investigated the effects of varying heat source temperatures and mass flow rates. They observed that when the heat source temperature changes rapidly, a power spike is produced by the TEG, hence rapid variations should be avoided to protect the electrical equipment.

1) Electro-Thermal Model Description: Consider the schematic of the TEG WHR system in Fig. 7. As exhaust gases enter the hot HEX, heat is transferred through the TEGs to the cold-side HEX. The model can be discretized in the flow direction to form a control volume (CV) around each TEG or p-n couple (see Fig. 7). Performing an energy balance on the CV, the rate of heat transfer for the exhaust gases (ΔQ_{source}) and the cooling fluid (ΔQ_{sink}) at steady-state are defined as

$$\Delta Q_{source} = \dot{m}_{exh} C_{p,exh} \left(T_{exh} - T_{out}\right) = Q_H \tag{6a}$$

$$\Delta Q_{sink} = \dot{m}_{w} C_{p,w} \left(T_{w,out} - T_{w}\right) = Q_C \tag{6b}$$

where $\dot{m}_{exh}$, $C_{p,exh}$, T_{exh}, and T_{out} are the mass flow rate, specific heat, inlet and outlet temperatures of the exhaust gas, respectively. The same is defined for the cooling fluid (T_w). Q_H is the heat rate entering the TEGs and Q_C is the heat rate exiting

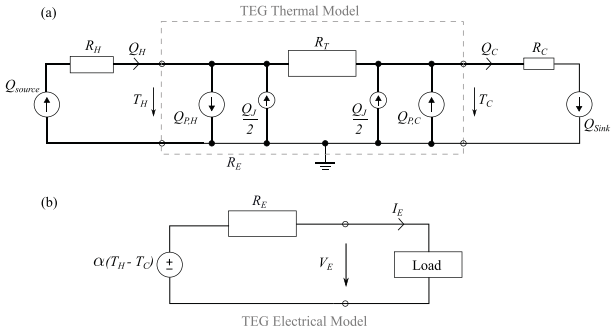

Fig. 8. (a) Electro-thermal equivalent circuit. (b) Electrical circuit.

the TEGs, with no power generation (or thermal losses) resulting in $Q_H = Q_C$.

The equivalent electro-thermal circuit of the TEG WHR system is shown in Fig. 8. There is an inherent temperature drop from the exhaust gases to the hot side temperature of the TEG (T_H) due to the heat exchanger thermal resistance. The heat transferred from the heat exchangers to the TEGs is calculated as

$$Q_H = \frac{T_{h,m} - T_H}{R_H} \tag{7a}$$

$$Q_C = \frac{T_C - T_{c,m}}{R_C} \tag{7b}$$

where $T_{h,m}$ is calculated as the average temperature of the inlet and outlet exhaust temperatures of the CV. $T_{c,m}$ is similarly defined and is the average temperature of the cooling fluid inlet and outlet. R_H and R_C are the thermal resistances of the hot HEX and cold HEX, respectively, over the CV.

Considering constant cross-sectional area of the p-n legs and material temperature-independent properties, the heat transferred through the TEG is calculated at each junction as [19]

$$Q_H = \alpha T_H I + \frac{T_H - T_C}{R_T} - \frac{1}{2} I^2 R_E \tag{8a}$$

$$Q_C = \alpha T_C I + \frac{T_H - T_C}{R_T} + \frac{1}{2} I^2 R_E \tag{8b}$$

The Peltier heat is defined as $Q_{P,H} = \alpha T_H I$ at the hot side, $Q_{P,C} = \alpha T_C I$ at the cold side and Joule heating, $Q_J = I^2 R_E$ reduces the temperature difference at the hot side and increases the temperature difference at the cold side [19]. These equations represent a lumped model of the spatially distributed effects within the TEG. R_T is the thermal resistance of the TEG module when there is no current flow. (8) should be multiplied by the total number of TEG modules in the CV for the correct energy balance of the system. From these equations, it is observed that the current flowing through the TEG affects the temperature difference across the TEG (Fig. 8a). Subtracting Q_C from Q_H the power output, P_E is derived as

$$P_E = \alpha(T_H - T_C)I - I^2 R_E. \tag{9}$$

If the TEGs are connected electrically in series, then the output voltage of each TEG is summed to calculate the power as

$$P_E = I \sum (V_E - I R_E). \tag{10}$$

A transient model may be created by adding heat capacity to each component (HEXs, exhaust gas, cooling fluid) for each equation described above and solving [8]

$$M C_p \frac{dT}{dt} = Q_{in} - Q_{out} \tag{11}$$

where M is the mass of the component in the CV, $\frac{dT}{dt}$ is the temperature rate of change in the CV, Q_{in} and Q_{out} are the heat transfer rate into and out of the CV, respectively. Transient models for TEG WHR have been implemented by [16], [62]. The TEG can assume negligible heat capacity since its electrical response time is magnitudes faster than the thermal response of the system and considered relatively instantaneous [60], [63]. Hussain *et al.* [64] developed a 1-D lumped mass transient model to investigate the potential of TEGs in a hybrid vehicle. Their simulation results indicated a 300–400 W power generation for a 2.5 L hybrid vehicle under a highway drive cycle.

B. Maximum Power Point Tracking

Power converters interface a TEG system with an electric load. In conventional and mild-hybrid drivetrains, the load is the low voltage subsystem that is connected to a lead-acid battery. In hybrid vehicles, the TEG system can also be connected to the high voltage battery. In both cases, an energy storage element is available. Hence, TEG systems are operated independent of any load characteristic (Fig. 5) and maximize the energy output of the TEG system (Fig. 8). In rare events, e.g. when the battery is fully charged and the electric load is low, the power is limited by reducing the TEG current I_E [65], [66]. *Maximum power point tracking* (MPPT) strategies maximize the electric power output for given boundary conditions, that are the heat transfer rate of the hot side and cold side heat exchangers as well as the thermal resistances of the system. MPPT strategies adjust the TEG current I_E (or alternatively the TEG terminal voltage V_E) to maximize the electrical power $P_E = V_E I_E$ according to the steady-state TEG characteristic shown in Fig. 5.

The MPP is located at $I_S/2$ (or alternatively $E/2$), where I_S is the short circuit voltage of the current, assuming that the open circuit voltage E and the resistance R_E are independent of the current. Hence, strategies have been proposed that estimate I_S and the MPP from the measurements [67]–[69]. However, the Seebeck coefficient α and the electric resistance R_E have temperature dependencies as shown in Table III. Hence, peak seeking strategies are gaining popularity. Examples are the *perturb and observe* (P&O) method [70]–[75], *incremental conductance* (IncCond) method [76]–[78], and *ripple correlation control* (RCC) including the *signal injection* method [79].

P&O operates inherently in discrete time where the sampling period T_s is chosen much larger than the electro-thermal time constants. At each time step, P&O varies the current setpoint I_E by a step ΔI_E either in positive or negative direction. If the power P_E has increased compared to the power of the last time step P_E^-, the setpoint is moved in the same direction. Alternatively, the setpoint is moved in the opposite direction. It is possible to write the concept in compact form as

$$I_E^+ = I_E + \text{sign}(P_E - P_E^-)\,(I_E - I_E^-), \tag{12}$$

where $\Delta I_E = I_E - I_E^-$, I_E^- is the current of the last time step, and I_E^+ is the setpoint applied in the next period. P&O (sometimes called hill-climb method) is a simple and effective strategy but requires trade-offs when choosing the parameters T_s and ΔI_E. A large T_s increases the time of convergence to the maximum power point. A small T_s increases the risk that electrothermal dynamics distort the power measurement due to stored energy and prevent P&O from identifying the steady-state peak. Furthermore, a sufficiently large ΔI_E is required that prevents measurement noise from affecting the power measurement. Ultimately, P&O identifies the MPP with suitable parameters but keeps moving around the MPP.In practice, this operation is typically acceptable since the MPP is a flat optimum.

The IncCond method is based on considering that the derivative of power with respect to current $\frac{dP_E}{dI_E}$ vanishes at the MPP, is positive on the left hand side of the MPP, and negative on the right hand side of the MPP.The derivative is

$$\frac{dP_E}{dI_E} = \frac{d(V_E I_E)}{dI_E} = V_E + I_E \frac{dV_E}{dI_E} \approx V_E + I_E \frac{\Delta V_E}{\Delta I_E}, \quad (13)$$

where the last approximation corresponds to a discretization with sampling time T_s with $\Delta V_E = V_E - V_E^-$ and $\Delta I_E = I_E - I_E^-$. Hence, the following qualifiers are obtained

$$\frac{dP_E}{dI_E} > 0 \;\Rightarrow\; \frac{\Delta V_E}{\Delta I_E} > -\frac{I_E}{V_E}, \quad (14a)$$

$$\frac{dP_E}{dI_E} = 0 \;\Rightarrow\; \frac{\Delta V_E}{\Delta I_E} = -\frac{I_E}{V_E}, \quad (14b)$$

$$\frac{dP_E}{dI_E} < 0 \;\Rightarrow\; \frac{\Delta V_E}{\Delta I_E} < -\frac{I_E}{V_E}. \quad (14c)$$

where (14a), (14b), (14c) corresponds to an operation point on the left hand side of the MPP, at the MPP, and on the right hand side of the MPP, respectively. Consequently, the current operation point I_E^+ is moved accordingly. In comparison to P&O, IncCond offers a more robust quantifier on the location of the operation point. Similarly to P&O, IncCond requires a sufficiently large step and keeps moving around the MPP.

Signal injection [79] is described as an example of various RCC methods. Signal injection adds a high frequency sinusoidal signal $\hat{i}_E = I_{hf} \sin(\omega_{hf})$ to an operation point, i.e. the TEG is operated at $i_e = I_E + \hat{i}_E$ where I_{hf} is the injection magnitude, $\omega_{hf} = 2\pi f_{hf}$ is the injection frequency, and f_{hf} is typically several Hz to several hundreds of Hz. The theory is based on the concept that $\hat{i}_E$ will result in a high frequency voltage response $\hat{v}_E$ that vanishes at the MPP, is in phase on the left hand side of the MPP, and out of phase on the right hand side of the MPP.The term $\hat{v}_E$ can be extracted from the voltage measurement $v_e = v_E + \hat{v}_E$ by high pass filtering. Multiplying $\hat{v}_E$ with $\hat{i}_E$ results in

$$\hat{p}_E = \hat{v}_E \hat{i}_E = V_{hf} I_{hf} \sin(\omega_{hf}) \sin(\omega_{hf} - \phi), \quad (15)$$

where V_{hf} is the magnitude of the high frequency voltage response and ϕ is the phase angle difference between the voltage and current signal. Applying trigonometric identities, the equation becomes

$$\hat{p}_E = V_{hf} I_{hf} \left(\cos(\phi) \sin^2(\omega_{hf}) + \sin(\phi) \sin(2\omega_{hf})/2 \right). \quad (16)$$

The first term in the brackets introduces an offset that is a function only of ϕ and can be extracted by low pass filtering since the second term in the brackets has a zero offset. The resulting mean value $\hat{\bar{p}}_E = V_{hf} I_{hf} \cos(\phi)/2$ is positive if the voltage is in phase ($\phi \in [-\frac{\pi}{2}, \frac{\pi}{2}]$), where the TEG is operated on the left hand side of the MPP and negative if the voltage is out of phase ($\phi \in [\frac{\pi}{2}, \frac{3\pi}{2}]$), where the TEG is operated on the right hand side of the MPP.Furthermore, the signal vanishes at the MPP where the injection magnitude V_{hf} tends to zero. Hence, $\hat{\bar{p}}_E$ can be used as control feedback to adjust the current setpoint through a proportional-integral (PI) controller. In comparison with $IncCond$ and $P\&O$, signal injection offers a robust quantifier on the location of the operation point and can converge to the exact MPP.

VI. Experimental Work

The first TEG WHR system experimentally investigated in the exhaust system of a vehicle was by Birkholz *et al*. in 1988. The TEG WHR system produced 58W when tested on a 944 Porsche, at maximum engine load [80]. Since then, other researchers as well as major automotive manufacturers have investigated waste heat recovery in vehicles through the use of thermoelectric generators. Funded by the U.S. Department of Energy (DOE), BMW and Ford designed a fully integrated TEG WHR system whose ultimate goal was to achieve a 10% gain in fuel efficiency for passenger vehicles [29]. Although they began with flat TEG modules, their design evolved to arranging the TEG couples in a cylindrical form. BMW also built an integrated TEG WHR system in the EGR cooler of a diesel vehicle with PbTe TEGs that produced a max power of ∼250W [89]. General Motors was funded separately by the DOE and explored Skutterudite flat TEGs [86]. Honda and Hyundai investigated TEG WHR systems for hybrid electric vehicle applications [90], [88].

The mentioned automotive companies had similar designs which included the exhaust gas HEX (rectangle, hexagon, etc.) in the center, TEGs attached to the outer surface of the exhaust HEX and coolant tubes or blocks on the outside of the system. Eventually BMW's thermoelectric manufacturing partner, Gentherm, changed their TEG WHR design where the coolant HEX was in the center, the TEGs on the perimeter of the coolant HEX and the exhaust gases flowed through the outside. The outcome of their second design, TEG "cartridges", had net zero fuel efficiency gains for a BMW X3 (2L turbocharged engine) for a US06 drive cycle due to the added weight of the system and because it was installed in the center muffler (exposed to lower temperatures). However, when a larger TEG system was installed immediately after the CC on a F350 (6.2L, V8) a fuel efficiency gain of 1.2% was achieved [91].

Table IV summarizes other achievements for TEG WHR systems in the literature. The work presented, is by researchers who experimentally evaluated the performance of their systems on engines and provided the maximum power generated. Engines were mostly tested under steady-state conditions and engine loads that resulted in high exhaust mass flow rates and temperatures from the engine. It should also be noted that different engine sizes result in different quantities of thermal losses available and large heavy-duty engines such as [28] can produce

TABLE IV
EXPERIMENTAL TEG WHR SYSTEM POWER OUTPUT REPORTED IN THE LITERATURE

Location	Engine	TEG Max Power [W]	Driving Conditions	Hot HEX	TEG Material/ Module	Cold HEX	Ref
Exhaust manifold	944 Porsche 2.7L	58	max engine load	square channel	$FeSi_2$	coolant block	[80]
Turbocharger exit	Cummins NTC350 14L	1068	300HP 1700 RPM	octagonal fins	HZ-13	coolant block	[81]
Exhaust manifold	3L	35.6	constant speed (60km/h, hill climb)	flat plate fins	SiGe	coolant block	[82]
After CC	1999 Sierra GMC 5.3L V8	130/255	constant speed (112.6km/h)/7.2% incline	offset strip fin	HZ-20	coolant block	[83]
Radiator	~ 2L	75	constant speed (80km/h)	tube block	Bi_2Te_3	heat pipes/fins	[84]
After CC	BMW 530i 3L 6cyl	605/450	constant speed (110kmh)/US06 drive cycle	fins in cylinder	half-Heusler /Bi_2Te_3	coolant tubes	[29]
After CC	2L	600	constant speed (125km/h)	"fishbone" finned	- -[a]	water block	[85]
After CC	Chevy Suburban 5.3L	57	US06 drive cycle	- -	Skutterudite	coolant block	[86]
Exhaust pipe	Caterpillar diesel	1000	constant mass flow (.48kg/s)	flat plate fins	half-Heusler	cold plate	[28]
Exhaust manifold	turbocharged diesel 4L 6cyl	119	constant 2000RPM (.6MPa BMEP)	flat plate fins	Bi_2Te_3	cold plate (finned structure)	[87]
After CC	Golf 1.4L TSI 4cyl	111/30	2000RPM, 85%FTTP /NEDC drive cycle	square channel	TEG1-12611-6.0	cold plate	[4]
Exhaust manifold	2L 4cyl SI for hybrid	98.8	constant 3000RPM .6MPa BMEP	hexagonal fins	1261G-7L31-05CQ	hexagonal fins	[88]

higher power output from a TEG WHR since the engines exhibit higher exhaust mass flow rates. Bass *et al*. [81] successfully recovered over 1kW of electrical power from a diesel truck engine after discovering that heat transfer enhancement was needed for their hot HEX design. Thacher *et al*. [83] quantified the parasitic losses of the TEG WHR system on an engine truck, by taking into account the rolling resistance due to the added weight and the back pressure of the HEX. At high speeds, the pressure drop across the hot HEX was actually lower than the system without the HEX due to lower exhaust mass flow rates caused by the increase in fuel efficiency. Almost 2% fuel efficiency gains were achieved at 120 km/h.

Although the majority of the research has focused on waste heat recovery from the exhaust gases, other locations have also been experimentally investigated. Kim *et al*. [84] took advantage of the fact that the radiator is already a HEX in the vehicle and installed heat pipes to transfer energy from the hot coolant to TEG modules. They calculated the electrical power efficiency to be 0.3% at a vehicle speed of 80kmh. Massaguer *et al*. [4] tested a small TEG WHR system on a Golf TSI engine and found that the TEGs produced lower power than expected during an NEDC drive cycle, but this was due to designing for the maximum expected temperature. However, once the system was redesigned for the most common temperature range in the NEDC drive cycle, different TEG modules were used and fins were added to their hot HEX design. The redesign is expected to achieve over 200 W in the NEDC drive cycle.

VII. FUTURE TRENDS

A. Advances in TE Materials/Modules

In the last decade, research into improving thermoelectric materials has made great strides [92]. Observing (3), low thermal conductivity (k) and high power factor ($\alpha^2\sigma$) is desirable for achieving high ZT values of TE materials. Techniques such as suppressing the mean-free path of phonons and optimizing carrier concentration has succeeded in doubling or tripling the ZT of some materials. The highest ZT value reported in the literature is 2.6 for an SnSe single crystal [93]. Other promising materials include BiCuSeO due to its low thermal conductivity, low cost, non-toxicity and thermal stability [92]. High temperature TE materials have also gained increasing interest [94], [95], since they are more suitable in the vehicle exhaust environment compared to the commonly used Bismuth Telluride modules. However, translating the added benefits of high temperature thermoelectrics from the material level to the module level has proven to be challenging. Stobart *et al.* [94] observed up to a 23% reduction in Seebeck coefficient as well as higher electrical and lower thermal resistance than expected as a result of the fabrication process. Bonding techniques continue to be an area of research as inefficient joining of the electrical contacts results in higher electrical resistance than desired. However, improvements continue to be made, a Bismuth Telluride/Skutterudite segmented module was recently manufactured and tested with 12% efficiency [96]. Improving thermoelectric materials and manufacturing techniques for thermoelectric modules is a highly intensive ongoing research topic and more in-depth reviews are found in [97], [98].

B. Higher System Integration

TEG WHR system performance not only depends on the available TE materials but also on the high integration with HEX design to optimize the power produced by the system. Currently, flat TEG modules are mounted on heat exchangers with thermal interface materials to reduce the contact thermal resistance between surfaces. These contact resistances contribute to losses in the overall system, thus a lower efficiency is achieved. Advances in additive manufacturing could potentially reduce or eliminate these losses. The researchers in [99], 3D printed Bismuth Telluride half rings and mounted them on a pipe (heat exchanger) with silver paste to demonstrate the potential of conformal-shape printed TEGs. As advances are made in the field of additive manufacturing, the potential of printing the TE p-n legs directly on

the surface of a heat exchanger would eliminate the contact resistances and shape-conforming TEGs would allow for more compact HEX designs, thus increasing the overall performance of a TEG WHR system in a vehicle.

Achieving a lower thermal resistance of the hot side HEX is also crucial for increasing the power output of the system. Although different heat transfer enhancement techniques have successfully been reported in the literature as were mentioned in Section IV-A, recently heat pipes are being investigated for increasing the heat transfer rate from the exhaust gases to the hot side of the TEG. Cao *et al*. [100] designed a system that utilized heat pipes and studied the heat transfer enhancement for varying heat pipe insertion depths and heat pipe angle with respect to the exhaust flow. They found that an insertion depth of 60mm and angle of 15° were optimal for enhancing the power output of the TEGs by 10.2%.

Li *et al*. [5] also employed heat pipes, but used them for both the hot side and cold side HEX. Their multiphysics model investigated a cylindrical TEG WHR system where heat pipes were placed in the radial direction and concentric TEG modules were used. Two configurations were studied, one with the exhaust flow through the center of the system (coolant flow through the outside) and the second with coolant through the center (exhaust flow through the outside). Their modeling results demonstrated that the system with exhaust flowing through the outside generated higher power since this increases the heat transfer area for the exhaust gas, which has a lower convective heat transfer than water. It should be noted that the studies with heat pipes for the hot HEX have limited the operating range to ∼250-270° C and further research is required for obtaining higher operating temperatures for heat pipes. However, this temperature limit is not a problem for the cold side HEX. Lv *et al*. [101] found that using heat pipes for cooling the cold side of the TEG resulted in a higher power output and lower cost compared to a finned-heat sink and a water-cooled block through their experimental study.

C. Transient System Design

A shift has been observed from analyzing TEG WHR systems for vehicle applications from a steady-state point of view to a transient design approach. As indicated in Table IV, the majority of the research has previously focused on testing TEG WHR systems at steady-state points of operation and when the systems are tested under transient conditions, the power output is lower than expected. However, by developing transient models the system may be analyzed for different driving conditions such as drive cycles.

A recent study by Massaguer *et al*. [4] demonstrated that if a TEG WHR recovery system is designed for the maximum power conditions, the system does not perform well under dynamic driving conditions. The reason being that maximum engine loads are not indicative of what occurs in real drive cycles. Their system was originally designed for the steady-state engine condition of 2000RPM and 85% full-throttle pedal position (FTTP) and produced 111W under these conditions. However, when the system was tested under the NEDC cycle, the maximum power produced was only 30W due to lower exhaust gas temperatures in the drive cycle. Also, Lead Telluride TEG modules used for their system have a lower performance at low temperatures. The system was redesigned for the most common temperature range of 260-380° C and more appropriate TEG modules made of Bismuth Telluride were used instead, where a bypass design concept was introduced to ensure the TEGs would not overheat at times in the drive cycle when this temperature was exceeded.

A dynamic model and experimental validation were presented by Lan *et al*. [62] for a 4-module TEG WHR system tested in the exhaust of a heavy-duty diesel truck engine. The goal was to create a model that could predict the performance of the TEG modules under transient conditions as well as for developing temperature control strategies by accurately predicting the exhaust exit temperature from the hot HEX. A model was created of a 20 TEG module system that was installed upstream of the Diesel Particulate Filter (DPF) and the hot HEX exit temperature had a requirement of 548K for the DPF to work appropriately. The authors also suggested a bypass solution to ensure the TEG modules would not exceed their temperature limit and to ensure the DPF performance was not degraded. A controller was implemented to the exhaust bypass valve and based on the measured exhaust inlet temperature, the dynamic model could predict the exhaust HEX exit temperature (inlet to the DPF).

D. Fuel Economy Metric

Although researchers have previously focused on maximum power produced by the TEG WHR system as a performance metric, recently there has been a trend towards evaluating the energy recovered by the system. Kim *et al*. [102] integrated the power produced by a TEG WHR system with 60 TEG modules for 4 different vehicle drive cycles to understand the performance of the system for each drive cycle. Taking into account the pumping losses for the cold side HEX, the integral of the net power generated over the integrated engine power during the drive cycle was used to calculate the energy % gain. The energy gains ranged from 1.54% (WLTC drive cycle) to 1.68% (FTP-75 drive cycle).

In [103], the authors proposed a method for evaluating the potential fuel economy gains as a function of the generated power of the TEG WHR system and the back pressure created by the system. They proposed either experimentally or numerically testing a TEG WHR system design at various engine operation points to derive a mathematical relationship between the power generated and back pressure imposed on the engine. This is done to determine a region where fuel economy is positive and to test if the proposed TEG WHR system will operate in this positive fuel economy region for most of the operating conditions of the engine. It is interesting to note that the maximum fuel economy point does not coincide with the maximum net power generation of the TEG WHR system. Yang *et al.* [104] have proposed a multi-objective optimization based on their transient TEG WHR system model. The objective is to minimize the number of TEG modules in the system while constraining the allowable pressure drop of the hot heat exchanger, to investigate the potential for fuel economy improvement.

Finally, there have been researchers not only investigating the feasibility of TEG WHR systems in passenger vehicles but also researching large heavy-duty truck applications. Since these vehicles have larger engines that produce higher thermal losses

and exhibit high exhaust mass flow rates, studies have been conducted into the feasibility of TEG WHR in these vehicles [3], [105].

VIII. Conclusion

The benefits of direct energy conversion and ability to operate under transient conditions have made thermoelectric generators a heavily researched topic for waste heat recovery in vehicles. In the last decades, as the ZT of thermoelectric materials has increased and promising thermoelectric materials have been discovered, there has been a growing interest in the implementation of TEGs in vehicles. However, more research is needed to translate these new materials from the laboratory to manufactured modules for higher efficiency. The efficiency of a TEG WHR system not only depends on the thermoelectric materials used but also on the high integration with the heat exchangers. Much research is being done on enhancing the heat transfer of the hot side HEX to improve the overall power output of the system. Although the maximum power produced by a TEG WHR system has been the focus of much of the research, recently researchers have investigated the transient operation of TEGs for varying drive cycles. Waste heat recovery in vehicles utilizing TEGs is an ongoing research topic and as advances are made not only in TEG module technology but also on the system integration, TEGs are a promising solution for increasing a vehicle's fuel economy.

References

[1] "Global EV Outlook 2017: Two million and counting," International Energy Agency, Paris, France, 2017. [Online]. Available: https://www.iea.org/publications/freepublications/publication/GlobalEVOutlook2017.pdf

[2] BNEF, "Electric vehicle outlook 2017," Bloomberg Finance, New York, NY, USA, Jul. 2017. [Online]. Available: https://data.bloomberglp.com/bnef/sites/14/2017/07/BNEF_EVO_2017_ExecutiveSummary.pdf

[3] N. Muralidhar, M. Himabindu, and R. V. Ravikrishna, "Modeling of a hybrid electric heavy duty vehicle to assess energy recovery using a thermoelectric generator," *Energy*, vol. 148, pp. 1046–1059, Apr. 2018.

[4] A. Massaguer *et al.*, "Transient behavior under a normalized driving cycle of an automotive thermoelectric generator," *Appl. Energy*, vol. 206, pp. 1282–1296, Nov. 2017.

[5] B. Li, K. Huang, Y. Yan, Y. Li, S. Twaha, and J. Zhu, "Heat transfer enhancement of a modularised thermoelectric power generator for passenger vehicles," *Appl. Energy*, vol. 205, pp. 868–879, Nov. 2017.

[6] Y. Wang, C. Dai, and S. Wang, "Theoretical analysis of a thermoelectric generator using exhaust gas of vehicles as heat source," *Appl. Energy*, vol. 112, pp. 1171–1180, Dec. 2013.

[7] Y. A. Cengel and M. A. Boles, *Thermodynamics: An Engineering Approach*, 5th ed. Boston, MA, USA: McGraw-Hill, 2006.

[8] F. P. Incropera, D. P. Dewitt, T. L. Bergman, and A. S. Lavine, *Fundamentals of Heat and Mass Transfer*, 6th ed. Hoboken, NJ, USA: Wiley, 2007.

[9] J. B. Heywood, *Internal Combustion Engine Fundamentals*. New York, NY, USA: McGraw-Hill, 1988, vol. 21.

[10] J. Lagrandeur, D. T. Crane, and B. Llc, "Vehicle fuel economy improvement through thermoelectric waste heat recovery," in *Proc. DEER Conf.*, Chicago, IL, Aug. 2005, pp. 1–24.

[11] D. Crane, "Potential thermoelectric application in diesel engine," in *Proc. 9th Diesel Engine Emissions Reduction Conf.*, Aug. 2003, pp. 1–6.

[12] M. Li, "Thermoelectric-generator-based DC-DC conversion network for automotive applications," Ph.D. dissertation, KTH, Stockholm, Sweden, 2011.

[13] F. Charles, D. Ewing, J. Becard, J.-S. Chang, and J. Cotton, "Optimization of the exhaust mass flow rate and coolant temperature for exhaust gas recirculation (EGR) cooling devices used in diesel engines," SAE, Troy, MI, USA, Tech. Paper 2005-01-0654, 2005.

[14] H. Wei, T. Zhu, G. Shu, L. Tan, and Y. Wang, "Gasoline engine exhaust gas recirculation—A review," *Appl. Energy*, vol. 99, pp. 534–544, 2012. [Online]. Available: http://dx.doi.org/10.1016/j.apenergy.2012.05.011

[15] C. Brace, H. Burnham-Slipper, R. S. Wijetunge, N. D. Vaughan, K. Wright, and D. Blight, "Integrated cooling systems for passenger vehicles," SAE, Troy, MI, USA, Tech. Paper 2001-01-1248, 2001.

[16] D. T. Crane, "An introduction to system-level, steady-state and transient modeling and optimization of high-power-density thermoelectric generator devices made of segmented thermoelectric elements," *J. Electron. Mater.*, vol. 40, no. 5, pp. 561–569, May 2011.

[17] T. A. Horst, W. Tegethoff, P. Eilts, and J. Koehler, "Prediction of dynamic Rankine Cycle waste heat recovery performance and fuel saving potential in passenger car applications considering interactions with vehicles' energy management," *Energy Convers. Manag.*, vol. 78, pp. 438–451, Feb. 2014.

[18] N. Espinosa, M. Lazard, L. Aixala, and H. Scherrer, "Modeling a thermoelectric generator applied to diesel automotive heat recovery," *J. Electron. Mater.*, vol. 39, no. 9, pp. 1446–1455, Sep. 2010.

[19] S. W. Angrist, *Direct Energy Conversion*, 4th ed. Boston, MA, USA: Allyn and Bacon, Inc., 1982.

[20] A. F. Ioffe, *Semiconductor Thermoelements and Thermoelectric Cooling*. London, U.K.: Infosearch Limited, 1957.

[21] K. Matsubara, "Development of a high efficient thermoelectric stack for a waste exhaust heat recovery of vehicles," in *Proc. ICT 21st Int. Conf. Thermoelectrics*, Long Beach, CA, Aug. 2002, pp. 418–423.

[22] D. Crane and J. Lagrandeur, "Automotive waste heat conversion to power program—2011 vehicle technologies program annual merit review," pp. 1–23, 2011.

[23] K. Biswas *et al.*, "High-performance bulk thermoelectrics with all-scale hierarchical architectures," *Nature*, vol. 489, no. 7416, pp. 414–418, Sep. 2012.

[24] A. U. Khan *et al.*, "Nano-micro-porous Skutterudites with 100% enhancement in ZT for high performance thermoelectricity," *Nano Energy*, vol. 31, pp. 152–159, Jan. 2017.

[25] C. Fu *et al.*, "Realizing high figure of merit in heavy-band p-type half-Heusler thermoelectric materials," *Nature Commun.*, vol. 6, pp. 1–7, Sep. 2015.

[26] W. Wei *et al.*, "Achieving high thermoelectric figure of merit in polycrystalline SnSe via introducing Sn vacancies," *J. Amer. Chem. Soc.*, vol. 140, no. 1, pp. 499–505, Jan. 2018.

[27] J. Lagrandeur, "Automotive waste heat conversion to electric power using Skutterudites, TAGS, PbTe, and Bi2Te3," in *Proc. 25th Int. Conf. Thermoelectrics*, Vienna, Austria, 2006, pp. 343–348.

[28] Y. Zhang *et al.*, "High-temperature and high-power-density nanostructured thermoelectric generator for automotive waste heat recovery," *Energy Convers. Manag.*, vol. 105, pp. 946–950, Sep. 2015.

[29] J. Lagrandeur and D. Crane, "Scientific and technical information (STI) for financial assistance and non-M&O/M&I," Amerigon, Irwindale, CA, USA, 2012. [Online]. Available: https://www.osti.gov/servlets/purl/1165358

[30] G. Min and D. M. Rowe, "Ring-structured thermoelectric module," *Semicond. Sci. Technol.*, vol. 22, no. 8, pp. 880–883, Jun. 2007.

[31] A. Bauknecht, T. Steinert, C. Spengler, and G. Suck, "Analysis of annular thermoelectric couples with nonuniform temperature distribution by means of 3-D multiphysics simulation," *J. Electron. Mater.*, vol. 42, no. 7, pp. 1641–1646, Jul. 2013.

[32] A. Schmitz, C. Stiewe, and E. Müller, "Preparation of ring-shaped thermoelectric legs from PbTe powders for tubular thermoelectric modules," *J. Electron. Mater.*, vol. 42, no. 7, pp. 1702–1706, Jul. 2013.

[33] C. Hadjistassou, E. Kyriakides, and J. Georgiou, "Designing high efficiency segmented thermoelectric generators," *Energy Convers. Manag.*, vol. 66, pp. 165–172, Feb. 2013.

[34] T. Ming, Y. Wu, C. Peng, and Y. Tao, "Thermal analysis on a segmented thermoelectric generator," *Energy*, vol. 80, pp. 388–399, Feb. 2015.

[35] D. T. Crane and L. E. Bell, "Progress towards maximizing the performance of a thermoelectric power generator," in *Proc. 25th Int. Conf. Thermoelectrics*, Vienna, Austria, Aug. 2006, pp. 11–16.

[36] M. Freunek, M. Müller, T. Ungan, W. Walker, and L. M. Reindl, "New physical model for thermoelectric generators," *J. Electron. Mater.*, vol. 38, no. 7, pp. 1214–1220, Jul. 2009.

[37] F. J. Lesage, É. V. Sempels, and N. Lalande-Bertrand, "A study on heat transfer enhancement using flow channel inserts for thermoelectric power generation," *Energy Convers. Manag.*, vol. 75, pp. 532–541, Nov. 2013.

[38] J. Pandit, M. Thompson, S. V. Ekkad, and S. T. Huxtable, "Effect of pin fin to channel height ratio and pin fin geometry on heat transfer performance for flow in rectangular channels," *Int. J. Heat Mass Transfer*, vol. 77, pp. 359–368, Oct. 2014.

[39] X. Liu, Y. Deng, K. Zhang, M. Xu, Y. Xu, and C. Su, "Experiments and simulations on heat exchangers in thermoelectric generator for automotive application," *Appl. Therm. Eng.*, vol. 71, no. 1, pp. 364–370, Oct. 2014.

[40] Z. Niu, H. Diao, S. Yu, K. Jiao, Q. Du, and G. Shu, "Investigation and design optimization of exhaust-based thermoelectric generator system for internal combustion engine," *Energy Convers. Manag.*, vol. 85, pp. 85–101, Sep. 2014.

[41] X. Wang and Y. Deng, "Research on and thermal performance of the heat exchanger in automotive exhaust-based thermoelectric generator," SAE, Troy, MI, USA, Tech. Paper 2014-01-2594, 2014.

[42] Y. Wang, S. Li, Y. Zhang, X. Yang, Y. Deng, and C. Su, "The influence of inner topology of exhaust heat exchanger and thermoelectric module distribution on the performance of automotive thermoelectric generator," *Energy Convers. Manag.*, vol. 126, pp. 266–277, Oct. 2016.

[43] X. Liu, Y. Deng, S. Chen, W. Wang, Y. Xu, and C. Su, "A case study on compatibility of automotive exhaust thermoelectric generation system, catalytic converter and muffler," *Case Stud. Therm. Eng.*, vol. 2, pp. 62–66, Mar. 2014.

[44] T. Ma *et al.*, "Numerical study on thermoelectric-hydraulic performance of a thermoelectric power generator with a plate-fin heat exchanger with longitudinal vortex generators," *Appl. Energy*, vol. 185, pp. 1343–1354, Jan. 2017.

[45] T. Wang, W. Wang, W. Luan, and S.-T. Tu, "Waste heat recovery through plate heat exchanger based thermoelectric generator system," *Appl. Energy*, vol. 136, pp. 860–865, Dec. 2014, pp. 1–5.

[46] T. J. Hendricks, "Integrated thermoelectric-thermal system resistance optimization to maximize power output in thermoelectirc energy recovery systems," in *Proc. Mater. Res. Soc. Symp.*, vol. 1642, May 2014.

[47] K. Oetringer, "Upgrading hybrid-vehicles with a thermoelectric generator," in *Proc. 9th Int. Conf. Ecological Vehicles Renew. Energies*, Monte-Carlo, Monaco, Mar. 2014, pp. 1–5.

[48] A. Montecucco, J. Siviter, and A. R. Knox, "The effect of temperature mismatch on thermoelectric generators electrically connected in series and parallel," *Appl. Energy*, vol. 123, pp. 47–54, Jun. 2014.

[49] S. LeBlanc, "Thermoelectric generators: Linking material properties and systems engineering for waste heat recovery applications," *Sustain. Mater. Technol.*, vol. 1, pp. 26–35, Dec. 2014.

[50] S. Wang, T. Xie, and H. Xie, "Experimental study of the effects of the thermal contact resistance on the performance of thermoelectric generator," *Appl. Therm. Eng.*, vol. 130, pp. 847–853, Feb. 2018.

[51] A. Z. Sahin and B. S. Yilbas, "The thermoelement as thermoelectric power generator: Effect of leg geometry on the efficiency and power generation," *Energy Convers. Manag.*, vol. 65, pp. 26–32, Jan. 2013.

[52] J.-H. Meng, X.-X. Zhang, and X.-D. Wang, "Multi-objective and multi-parameter optimization of a thermoelectric generator module," *Energy*, vol. 71, pp. 367–376, Jul. 2014.

[53] X. Liang, X. Sun, H. Tian, G. Shu, Y. Wang, and X. Wang, "Comparison and parameter optimization of a two-stage thermoelectric generator using high temperature exhaust of internal combustion engine," *Appl. Energy*, vol. 130, pp. 190–199, Oct. 2014.

[54] C. Wu, "Analysis of waste-heat thermoelectric power generators," *Appl. Therm. Eng.*, vol. 16, no. 1, pp. 63–69, Jan. 1996.

[55] Y. Hsiao, W. Chang, and S. Chen, "A mathematic model of thermoelectric module with applications on waste heat recovery from automobile engine," *Energy*, vol. 35, no. 3, pp. 1447–1454, Mar. 2010.

[56] S. Vale, L. Heber, P. Coelho, and C. Silva, "Parametric study of a thermoelectric generator system for exhaust gas energy recovery in diesel road freight transportation," *Energy Convers. Manag.*, vol. 133, pp. 167–177, Feb. 2017.

[57] R. J. Stevens, S. J. Weinstein, and K. S. Koppula, "Theoretical limits of thermoelectric power generation from exhaust gases," *Appl. Energy*, vol. 133, pp. 80–88, Nov. 2014.

[58] E. Massaguer, A. Massaguer, L. Montoro, and J. R. Gonzalez, "Modeling analysis of longitudinal thermoelectric energy harvester in low temperature waste heat recovery applications," *Appl. Energy*, vol. 140, pp. 184–195, Feb. 2015.

[59] W. He, S. Wang, Y. Zhao, and Y. Li, "Effects of heat transfer characteristics between fluid channels and thermoelectric modules on optimal thermoelectric performance," *Energy Convers. Manag.*, vol. 113, pp. 201–208, Apr. 2016.

[60] J. H. Meng, X. X. Zhang, and X. D. Wang, "Dynamic response characteristics of thermoelectric generator predicted by a three-dimensional heat-electricity coupled model," *J. Power Sources*, vol. 245, pp. 262–269, Jan. 2014.

[61] X. Gou, S. Yang, H. Xiao, and Q. Ou, "A dynamic model for thermoelectric generator applied in waste heat recovery," *Energy*, vol. 52, pp. 201–209, Apr. 2013.

[62] S. Lan, Z. Yang, R. Chen, and R. Stobart, "A dynamic model for thermoelectric generator applied to vehicle waste heat recovery," *Appl. Energy*, vol. 210, pp. 327–338, Jan. 2018.

[63] L. Chen, D. Cao, Y. Huang, and F. Z. Peng, "Modeling and power conditioning for thermoelectric generation," in *Proc. IEEE Annu. Power Electron. Specialists Conf.*, Rhodes, Greece, Jun. 2008, pp. 1098–1103.

[64] Q. E. Hussain, D. R. Brigham, and C. W. Maranville, "Thermoelectric exhaust heat recovery for hybrid vehicles," *SAE Int. J. Engines*, vol. 2, no. 1, pp. 1132–1142, 2009.

[65] R.-Y. Kim and J.-S. Lai, "A seamless mode transfer maximum power point tracking controller for thermoelectric generator applications," *IEEE Trans. Power Electronics*, vol. 23, no. 5, pp. 2310–2318, Sep. 2008.

[66] R.-Y. Kimg and J.-S. Lai, "Aggregated modeling and control of a boost-buck cascade converter for maximum power point tracking of a thermoelectric generator," in *Proc. 23rd Annu. IEEE Appl. Power Electronics Conf. Expo.*, Austin, TX, Feb. 2008, pp. 1754–1760.

[67] H. Wu, K. Sun, M. Chen, and Y. Xing, "Evaluation of power conditioning architectures for energy production enhancement in thermoelectric generator systems," *J. Electron. Mater.*, vol. 43, no. 6, pp. 1567–1573, Jun. 2013.

[68] H. Yamada, K. Kimura, T. Hanamoto, T. Ishiyama, T. Sakaguchi, and T. Takahashi, "A MPPT control method of thermoelectric power generation with single sensor," in *Power Electron. Drive Syst.*, Kitakyushu, Japan, Apr. 2013, pp. 545–558.

[69] I. Laird and D. D. C. Lu, "High step-up DC/DC topology and MPPT algorithm for use with a thermoelectric generator," *IEEE Trans. Power Electron.*, vol. 28, no. 7, pp. 3147–3157, 2013.

[70] H. Nagayoshi, K. Tokumisu, and T. Kajikawa, "Evaluation of multi MPPT thermoelectric generator system," in *Proc. 26th Int. Conf. Thermoelectrics*, Jeju Island, South Korea, Jun. 2007, pp. 318–321.

[71] H. Yamada, K. Kimura, T. Hanamoto, T. Ishiyama, T. Sakaguchi, and T. Takahashi, "A novel MPPT control method of thermoelectric power generation using state space averaging method," in *Proc. IEEE 9th Int. Conf. Power Electron. Drive Syst.*, Singapore, Dec. 2011, pp. 895–900.

[72] A. Hidaka, T. Tsuji, and S. Matsumoto, "A thermoelectric power generation system with ultra low input voltage boost converter with maximum power point tracking," in *Proc. Int. Conf. Renewable Energy Res. Appl.*, Nagasaki, Japan, Nov. 2012, pp. 1–5.

[73] J. Park and S. Kim, "Maximum power point tracking controller for thermoelectric generators with peak gain control of boost DC-DC converters," *J. Electron. Mater.*, vol. 41, no. 6, pp. 1242–1246, Jun. 2012.

[74] N. Kimura, "DC-DC converter current measurement by using FET on-state resistance for low-cost maximum power point tracking," in *Proc. IEEE 14th Workshop Control Model. for Power Electron.*, Salt Lake City, UT, USA, Jun. 2013, pp. 1–5.

[75] C. Vadstrup, E. Schaltz, and M. Chen, "Individual module maximum power point tracking for thermoelectric generator systems," *J. Electron. Mater.*, vol. 42, no. 7, pp. 2203–2208, Jul. 2013.

[76] R. Y. Kim and J. S. Lai, "Optimal design of adaptive maximum-power-point tracking algorithm for thermoelectric based battery energy storage system," in *Proc. 34th Annu. Conf. IEEE Ind. Electron. Soc.*, Orlando, FL, USA, Nov. 2008, pp. 861–866.

[77] R.-Y. Kim, J.-S. Lai, B. York, and A. Koran, "Analysis and design of maximum power point tracking scheme for thermoelectric battery energy storage system," *IEEE Trans. Ind. Electron.*, vol. 56, no. 9, pp. 3709–3716, Sep. 2009.

[78] F. Liu, S. Duan, F. Liu, B. Liu, and Y. Kang, "A variable step size INC MPPT method for PV systems," *IEEE Trans. Ind. Electron.*, vol. 55, no. 7, pp. 2622–2628, Jul. 2008.

[79] R. Rodriguez, M. Preindl, A. Emadi, and J. Cotton, "Maximum power point tracking for thermoelectric generators with high frequency injection," in *Proc. 41st Annu. Conf. IEEE Ind. Electron. Soc.*, Yokohama, Japan, Nov. 2015, pp. 004127–004132.

[80] U. Birkholz, E. Grob, U. Stohrer, and K. Voss, "Conversion of waste exhaust heat in automobiles using FeSi2 thermoelements," in *Proc. 7th Int. Conf. Thermoelectric Energy Convers.*, Arlington, VA, 1988, pp. 124–128.

[81] J. C. Bass, N. B. Elsner, and F. A. Leavitt, "Performance of the 1 kW thermoelectric generator for diesel engines," in *Proc. 13th Int. Conf. Thermoelectrics*, Kansas City, MO, USA, 1995, vol. 316, pp. 295–298.

[82] K. Ikoma, M. Munekiyo, K. Furuya, M. Kobayashi, T. Izumi, and K. Shinohara, "Thermoelectric module and generator for gasoline engine vehicles," in *Proc. 17th Int. Conf. Thermoelectrics*, Ngoya, Japan, May 1998, pp. 464–467.

[83] E. F. Thacher, B. T. Helenbrook, M. a. Karri, and C. J. Richter, "Testing of an automobile exhaust thermoelectric generator in a light truck," *Proc. Institution Mech. Engineers, Part D: J. Automobile Eng.*, vol. 221, pp. 95–107, Jan. 2007.
[84] S. Kim, S. Park, S. Kim, and S. H. Rhi, "A thermoelectric generator using engine coolant for light-duty internal combustion engine-powered vehicles," *J. Electron. Mater.*, vol. 40, no. 5, pp. 812–816, May 2011.
[85] X. Liu, Y. D. Deng, Z. Li, and C. Q. Su, "Performance analysis of a waste heat recovery thermoelectric generation system for automotive application," *Energy Convers. Manag.*, vol. 90, pp. 121–127, Jan. 2015.
[86] G. P. Meisner, "Skutterudite thermoelectric generator for automotive waste heat recovery," in *Proc. 3rd Thermoelectrics Appl.* Workshop, Baltimore, MD, USA: U.S. Dept. Energy, 2012. [Online]. Available: https://www.energy.gov/sites/prod/files/2014/03/f10/meisner.pdf
[87] T. Y. Kim, A. A. Negash, and G. Cho, "Waste heat recovery of a diesel engine using a thermoelectric generator equipped with customized thermoelectric modules," *Energy Convers. Manag.*, vol. 124, pp. 280–286, Sep. 2016.
[88] T. Y. Kim, J. Kwak, and B.-w. Kim, "Energy harvesting performance of hexagonal shaped thermoelectric generator for passenger vehicle applications: An experimental approach," *Energy Convers. Manag.*, vol. 160, pp. 14–21, Mar. 2018.
[89] A. Eder and M. Linde, *Efficient and Dynamic – the BMW Group Roadmap for the Application of Thermoelectric Generators.* pp. 1–23, 2011.
[90] M. Mori, T. Yamagami, M. Sorazawa, T. Miyabe, S. Takahashi, and T. Haraguchi, "Simulation of fuel economy effectiveness of exhaust heat recovery system using thermoelectric generator in a series hybrid," *SAE Int. J. Mater. Manuf.*, vol. 4, no. 1, pp. 1268–1276, 2011.
[91] V. G. Jovovic, "U.S. department of energy scientific and technical information (STI) for financial assistance and non-M&O/M&I project title: Thermoelectric waste heat recovery program for passenger vehicles," Gentherm LLC, Azusa, CA, USA, 2016. [Online]. Available: https://www.osti.gov/servlets/purl/1337561
[92] X. Zhou *et al.*, "Routes for high-performance thermoelectric materials," *Mater. Today*, vol. 21, no. 9, pp. 1–15, Nov. 2018.
[93] L.-D. Zhao *et al.*, "Ultralow thermal conductivity and high thermoelectric figure of merit in SnSe crystals," *Nature*, vol. 508, no. 7496, pp. 373–377, Apr. 2014.
[94] R. Stobart and Z. Yang, "The development of Skutterudite-based thermoelectric generators for vehicles," SAE, Troy, MI, USA, Tech. Paper 2018-01-0788, pp. 1–10, 2018.
[95] J. Szybist, S. Davis, J. Thomas, and B. Kaul, "Performance of a half-Heusler thermoelectric generator for automotive application," SAE, Troy, MI, USA, Tech. Paper 2018-01-0054, pp. 1–9, 2018.
[96] Q. Zhang *et al.*, "Realizing a thermoelectric conversion efficiency of 12% in bismuth telluride/Skutterudite segmented modules through full-parameter optimization and energy-loss minimized integration," *Energy Environ. Sci.*, vol. 10, no. 4, pp. 956–963, Apr. 2017.
[97] Q. H. Zhang, X. Y. Huang, S. Q. Bai, X. Shi, C. Uher, and L. D. Chen, "Thermoelectric devices for power generation: Recent progress and future challenges," *Adv. Eng. Mater.*, vol. 18, no. 2, pp. 194–213, Feb. 2016.
[98] L. Yang, Z. G. Chen, M. S. Dargusch, and J. Zou, "High performance thermoelectric materials: Progress and their applications," *Adv. Energy Mater.*, vol. 8, no. 6, pp. 1–28, Feb. 2018.
[99] F. Kim *et al.*, "3D printing of shape-conformable thermoelectric materials using all-inorganic Bi2Te3-based inks," *Nature Energy*, vol. 3, no. 4, pp. 301–309, 2018. [Online]. Available: http://dx.doi.org/10.1038/s41560-017-0071-2
[100] Q. Cao, W. Luan, and T. Wang, "Performance enhancement of heat pipes assisted thermoelectric generator for automobile exhaust heat recovery," *Appl. Therm. Eng.*, vol. 130, pp. 1472–1479, Feb. 2018.
[101] S. Lv *et al.*, "Study of different heat exchange technologies influence on the performance of thermoelectric generators," *Energy Convers. Manag.*, vol. 156, pp. 167–177, Jan. 2018.
[102] T. Y. Kim and J. Kim, "Assessment of the energy recovery potential of a thermoelectric generator system for passenger vehicles under various drive cycles," *Energy*, vol. 143, pp. 363–371, Jan. 2018.
[103] A. Massaguer *et al.*, "A method to assess the fuel economy of automotive thermoelectric generators," *Appl. Energy*, vol. 222, pp. 42–58, Jul. 2018.
[104] Z. Yang, R. Stobart, S. Lan, B. Mason, and W. Edward, "Towards optimal performance of a thermoelectric generator for exhaust waste heat recovery from an automotive engine," SAE, Troy, MI, USA, Tech. Paper 2018-01-0050, pp. 1–8, 2018.
[105] Y. D. Deng, T. Hu, C. Q. Su, and X. H. Yuan, "Fuel economy improvement by utilizing thermoelectric generator in heavy-duty vehicle," *J. Electron. Mater.*, vol. 46, no. 5, pp. 3227–3234, May 2017.

Romina Rodriguez received the B.S. and M.S. degrees in mechanical engineering from the University of California, Berkeley, CA, USA. She is a Ph.D. Candidate at the Mechanical Engineering Department, McMaster University, Hamilton, ON, Canada. She was a Mechanical Engineer with the Thermal Design & Analysis Group at Northrop Grumman between 2012 and 2014. Her research interests include energy conversion, thermal management, and thermoelectric generators.

Matthias Preindl (S'12–M'15–SM'18) received the B.Sc. degree in electrical engineering (*summa cum laude*) from the University of Padua, Padua, Italy, the M.Sc. degree in electrical engineering and information technology from ETH Zurich, Zurich, Switzerland, and the Ph.D. degree in energy engineering from the University of Padua, in 2008, 2010, and 2014, respectively. He was an R&D Engineer of Power Electronics and Drives at Leitwind AG, Sterzing, Italy (2010–2012), a Postdoctoral Research Associate with the McMaster Institute for Automotive Research and Technology, McMaster University, Hamilton, ON, Canada (2014–2015), and a Sessional Professor with the Department of Electrical and Computer Engineering, McMaster University (2015). He is currently an Assistant Professor with the Department of Electrical Engineering, Columbia University, New York, NY, USA. He received the Career Award of the Futura Foundation in South Tyrol, Italy, and the Career Award of the US National Science Foundation (NSF) in 2016 and 2017, respectively.

James S. Cotton is a Professor with the Department of Mechanical Engineering, McMaster University, Hamilton, ON, Canada, and the Associate Director of the McMaster Institute for Energy Studies, McMaster University. He is a Leading Researcher in energy harvesting and in the emerging fields of thermal energy recovery, storage, and electrohydrodynamics. His research interests include on developing, modeling, and experimentally validating technologies to advance efficient thermal management solutions and integrated community energy and harvesting systems.

Ali Emadi (S'98–M'00–SM'03–F'13) received the B.S. and M.S. degrees in electrical engineering with highest distinction from the Sharif University of Technology, Tehran, Iran, in 1995 and 1997, respectively, and the Ph.D. degree in electrical engineering from Texas A&M University, College Station, TX, USA, in 2000. He is the Canada Excellence Research Chair in Hybrid Powertrain, McMaster University, Hamilton, ON, Canada. Before joining McMaster University, he was the Harris Perlstein Endowed Chair Professor of Engineering and Director of the Electric Power and Power Electronics Center and Grainger Laboratories at the Illinois Institute of Technology, Chicago, IL, USA. He was the Founder, Chairman, and President of Hybrid Electric Vehicle Technologies, Inc. (HEVT) a university spin-off company of Illinois Tech. He is the principal author/co-author of over 450 journal and conference papers as well as several books. Dr. Emadi was the Inaugural General Chair of the 2012 IEEE Transportation Electrification Conference and Expo (ITEC) and has chaired several IEEE and SAE conferences in the areas of vehicle power and propulsion. He is the Founding Editor-in-Chief of the IEEE TRANSACTIONS ON TRANSPORTATION ELECTRIFICATION.